Astronomical and Astrophysical Transactions (*AApTr*), 2021, Vol. 32, Issue 4, pp. 355–370,
ISSN 1055-6796, Photocopying permitted by license only, ©Cambridge Scientific Publishers

Modified version of IDA software and its application to the study of the motion of asteroid 2007 PR10

T.Yu. Galushina*, O.N. Letner

Tomsk State University, 36 Lenin Avenue, Tomsk, 634050, Russia

Received 29 June, 2021

The paper presents a description of the modified *IDA* software. The algorithms for determining the Yarkovsky effect parameter, processing of radar observations, the ability of ephemeris DE438 use and conversion from the ephemeris time ET to the terrestrial time TT were added to the software. Two new subsystems *OMEGNO* (Orthogonal Mean Exponential Growth factor of Nearby Orbits) and *Secular resonances* were developed. Also, we included in the *IDA* software the automation of some processes described in detail in the paper. Using the modified *IDA* software, the dynamics of asteroid 2007 PR10 with a small perihelion distance has been studied. It was shown that the Yarkovsky effect influences the evolution of the asteroid's semimajor axis and the behaviour of the confidence domain of 2007 PR10. The signs of chaoticity in asteroid motion were investigated using the OMEGNO parameter, and all apsidal-nodal resonances to the 6th order inclusive were revealed.

Keywords: Software, dynamical evolution, Yarkovsky effect, OMEGNO, secular resonances, asteroid 2007 PR10

1 Introduction

The prediction of the motion of asteroids, particularly, near-Earth asteroids (NEA), is a complex problem that calls for the development of program complexes. They are usually based on numerical algorithms that overcome some difficulties associated with the peculiarities of asteroid motion. At present there are many algorithms and programs intended for a comprehensive study of asteroid dynamics, but not all programs are free.

Among the most well-known software systems, we should mention the online system *HORIZONS* (http://ssd.jpl.nasa.gov/horizons.cgi) and three Russian systems: the software package *EPOS* (L'vov and Tsekmeister, 2012), the multipurpose software package *AMPLE* (Novikov et al., 2009) and the software complex *IDA* developed at Scientific Research Tomsk State University (Galushina et al., 2019).

*Email: tanastra@nxt.ru

The *IDA* software (Investigation of the Dynamics of Asteroids) is intended for studying the dynamics and probabilistic orbital evolution of asteroids. The software complex can be used to predict asteroid motion at a given time, to construct the probabilistic orbital evolution, to study some peculiarities of asteroid motion, including close approaches, secular and orbital resonances with planets, Pluto and the Moon, and to reveal signs of chaoticity of motion. The *IDA* version described in (Galushina et al., 2019) has been changed significantly. Therefore, in the present work we describe in detail additional algorithms and programs and use the modified software complex to study the dynamics of NEA 2007 PR10 with a small perihelion distance ($q = 0.13$ AU).

2 Previous version of *IDA* software complex

The *IDA* software described in (Galushina et al., 2019) included subsystems *Assol*, *Observations*, *Distribution*, *Clone ensemble*, *Evolution* and *MEGNO*. Each subsystem solved a particular astronomical problem. Let us dwell a little more on each of them.

The *Assol* subsystem allows us not only to study the orbital evolution of the nominal orbit, but also to visualize the motion of an asteroid and large planets on a computer screen. The *Observations* subsystem fits the asteroid orbit to positional observations, determines the nonlinearity coefficient and constructs the initial confidence region using nonlinear methods. The *Distribution* subsystem visualizes the distribution of observations along the asteroid orbit. The *Clone ensemble* subsystem builds the ensemble of clones from the initial confidence region by linear methods based on the coordinates and velocity components of the nominal orbit and the covariance matrix calculated using the *Observations* subsystem. The *Evolution* subsystem studies the mean motion evolution and detects such peculiarities of motion as close approaches and orbital resonances with large planets, Pluto and the Moon. Finally, the *MEGNO* subsystem builds the evolution of the chaoticity parameter MEGNO (Mean Exponential Growth factor of Nearby Orbits) of asteroids.

The *IDA* software implements a numerical model of asteroid motion using formulas of the perturbed two-body problem. A detailed description of the employed algorithms, methods, stages of subsystem operations and input and output files is presented in (Galushina et al., 2019). The capabilities of the software complex and the results of its application were demonstrated in the example of studying the dynamics of asteroid 2012 MF7.

3 Algorithms added to IDA software

At the present time, the following algorithms and capabilities have been added to the *IDA* software:

- algorithms for determining the Yarkovsky effect (YE) parameter and its account in the construction of the orbital evolution;
- processing of radar observations;
- application of new planet ephemeris DE438;

- conversion from the ephemeris time ET to the modern terrestrial time TT;
- *OMEGNO* subsystem (Orthogonal Mean Exponential Growth factor of Nearby Orbits) used to detect the chaoticity of motion and to evaluate the predictability period;
- *Secular resonances* subsystem intended to detect and to construct the evolution of the resonance characteristics of apsidal-nodal resonances with the major planets and Pluto;
- automation of procedures of orbit fitting and generating clone ensembles, assessing the influence of perturbing factors on asteroid dynamics, adjusting the transverse acceleration component to take into account the Yarkovsky effect and drawing a large number of graphs.

Because of the significant changes in the *IDA* software, we consider it necessary to describe below the modified version of the software complex intended for a more qualitative study of asteroid dynamics.

3.1 Algorithm for determining the Yarkovsky effect parameter

The Yarkovsky effect characterizes the additional acceleration of the asteroid due to anisotropic thermal emission from its rough surface heated during the daytime and cooled at night. To take this effect into account, we need to know the physical properties and the rotation parameters of asteroids that are known only for a small number of objects. For the remaining asteroids, the coefficient is adjusted from observations to determine acceleration to take into account the Yarkovsky effect (Farnocchia et al., 2013). The acceleration is written in the form

$$a_{YE} = \frac{A}{r^2}, \tag{1}$$

where r is the heliocentric distance to the asteroid and A is the Yarkovsky effect coefficient. The acceleration given by Eq. (1) is added to the right side of the differential equations of asteroid motion. The precision of modern observations allows us to determine at best only the transverse acceleration component A_2. The *IDA* software implements two methods for determining this parameter by minimization of the mean squared error of observations.

The first method consists in varying the transverse acceleration parameter A_2 within a fixed interval with a given step. For each parameter value, the least squares problem is solved, and the mean squared error σ is calculated. The value of the transverse acceleration parameter A_2 that corresponds to the minimum σ value is the desired one. The observations are preliminarily rejected according to the three sigma rule using the model without the Yarkovsky effect. The obtained set of observations is used for further variation of the parameter A_2. The disadvantage of this method is that we are limited by the boundaries of the interval of values under study and the discrete step. In addition, much time is required to solve the least squares problem (Galushina and Letner, 2020).

The second method determines the parameter A_2 by joint integration of the motion equations, the equation for A_2 and the partial differential equations. The parameter A_2 is included in the number of the estimated parameters along with the coordinates

and the velocity components. The advantage of this approach is not only the higher calculation speed, but also the obtained uncertainties of the resulting value (Galushina and Syusina, 2020).

3.2 Processing of radar observations

When fitting the asteroid orbit, not only optical but also radar observations can be used. We have added this option to the *IDA* software to improve the accuracy of determining the parameter A_2. The problem of minimizing the objective function by fitting the object orbit to positional and radar observations can be written in the form

$$\Phi = w_i^2 \sum_{i=1}^{N} \left(\Delta\alpha_i^2 \cos^2 \delta_i^* + \Delta\delta_i^2\right) + \sum_{i=1}^{N_\tau} p_i^2 \Delta\tau_i^2 + \sum_{i=1}^{N_f} u_i^2 \Delta f_i^2 \to min, \qquad (2)$$

where $\Delta\alpha_i = \alpha_i(\hat{q}) - \alpha_i^*$ and $\Delta\delta_i = \delta_i(\hat{q}) - \delta_i^*$ are the differences between the calculated and measured values during the right ascension and declination, respectively; N is the number of positional measurements; $\Delta\tau_i = \tau_i(\hat{q}) - \tau_i^*$ are the differences between the calculated and measured signal time delays; $\Delta f_i = f_i(\hat{q}) - f_i^*$ are the differences between the calculated and measured Doppler frequency shifts; N_τ and N_f are the numbers of measurements of the signal time delays and of the Doppler frequency shifts; w_i, p_i and u_i are the weights of the angular measurements and measurements of time delays and of the Doppler frequency shifts, respectively; and $\hat{q} = (x, y, z, \dot{x}, \dot{y}, \dot{z})$ is the least squares estimate of the asteroid orbital parameters. The formulas for calculating the time delay, the Doppler frequency shift and their derivatives were taken from (Yeomans et al., 1992).

It should be noted that the use of radar observations imposes increased demands on the accuracy of numerical modelling. Therefore, we have made the following modifications of the IDA software. First, we added the new planet ephemeris DE438, and second, the conversion from the ephemeris time ET to the modern terrestrial time TT.

3.3 Algorithm for revealing and studying the secular resonances in the asteroid dynamics

The secular resonances are the resonances caused by commensurability between the precession velocities of the asteroid and planet orbits. The problem of revealing the secular resonances in the NEA dynamics is poorly understood because of the fast-changing behaviour of asteroids due to close and/or multiple approaches to the major planets, while secular resonances, as is well known, are observed for long time periods (Murray and Dermott, 1999). Nevertheless, the study of the secular resonances plays an important role in the dynamics of asteroids since the overlap of resonances, especially in the presence of at least one unstable resonance among them, may lead to chaoticity of their motion (Chirikov, 1979; Galushina and Sambarov, 2017; Aleksandrova et al., 2020). As characteristics of the secular resonance, the resonant argument

$$\psi = (l - 2p')\omega' - (l - 2p)\omega - \bar{m}(\Omega - \Omega'), \qquad (3)$$

and its first time derivative $\dot{\psi}$, the so-called resonant relationship, are considered. In formula (3), ω and Ω are the argument of the perihelion and the longitude of the ascending node of the asteroid orbit; ω' and Ω' are the same elements of the orbit of the perturbing body; and l, p, p' and $\bar{m}$ are integers.

A resonance arises when the resonant relationship is close to zero. The phenomenon when the resonant relationship is strictly equal to zero is called the sharp or exact resonance. The detailed algorithm for calculating the secular resonance characteristics is presented in (Bordovitsyna et al., 2012; Bordovitsyna et al., 2014; Galushina and Sambarov, 2017; Letner and Galushina, 2019).

Adjusting values of integers l, p, p' and $\bar{m}$, we obtain a spectrum of values of the resonant argument and the resonant relationship corresponding to it. In the *Secular resonances* subsystem we realized a set of apsidal-nodal resonances to the 6th order inclusive, namely, 20 resonant arguments and 20 resonant relationships corresponding to them. Table 1 presents these resonant relationships expressed as formulas. For convenience, we designated them as follows: formulas 1–16 describe the mixed (apsidal-nodal) secular resonances, formula 17 describes the pure nodal resonance, formulas 18 and 19 are for the apsidal resonances. Relationship 20 represents the geometrical Lidov–Kozai resonance.

Table 1 Types of apsidal-nodal resonant relationships to the 6th order inclusive.

No.	Type of the resonant relationship	No.	Type of the resonant relationship
1	$(\dot{\Omega} - \dot{\Omega}'_i) + \dot{\omega} - \dot{\omega}'_i$	11	$(\dot{\Omega} - \dot{\Omega}'_i) + \dot{\omega}$
2	$(\dot{\Omega} - \dot{\Omega}'_i) - \dot{\omega} + \dot{\omega}'_i$	12	$(\dot{\Omega} - \dot{\Omega}'_i) - \dot{\omega}$
3	$(\dot{\Omega} - \dot{\Omega}'_i) + 2\dot{\omega} - 2\dot{\omega}'_i$	13	$(\dot{\Omega} - \dot{\Omega}'_i) + \dot{\omega}'_i$
4	$(\dot{\Omega} - \dot{\Omega}'_i) - 2\dot{\omega} + 2\dot{\omega}'_i$	14	$(\dot{\Omega} - \dot{\Omega}'_i) - \dot{\omega}'_i$
5	$(\dot{\Omega} - \dot{\Omega}'_i) + \dot{\omega} + \dot{\omega}'_i$	15	$(\dot{\Omega} - \dot{\Omega}'_i) - 2\dot{\omega}'_i$
6	$(\dot{\Omega} - \dot{\Omega}'_i) - \dot{\omega} - \dot{\omega}'_i$	16	$(\dot{\Omega} - \dot{\Omega}'_i) + 2\dot{\omega}'_i$
7	$(\dot{\Omega} - \dot{\Omega}'_i) + 2\dot{\omega} + 2\dot{\omega}'_i$	17	$(\dot{\Omega} - \dot{\Omega}'_i)$
8	$(\dot{\Omega} - \dot{\Omega}'_i) - 2\dot{\omega} - 2\dot{\omega}'_i$	18	$\dot{\omega} - \dot{\omega}'_i$
9	$(\dot{\Omega} - \dot{\Omega}'_i) + 2\dot{\omega}$	19	$\dot{\omega} + \dot{\omega}'_i$
10	$(\dot{\Omega} - \dot{\Omega}'_i) - 2\dot{\omega}$	20	$\dot{\omega}$

We can determine the presence or absence of a secular resonance from the behaviour of the resonant characteristics. If the oscillations of the resonant argument are always strictly less than 360°, the libration of the argument takes place, the resonant relationship oscillates around the zero value, and the resonance is defined as stable. In the opposite case, when the resonant argument changes from 0 to 360°, its behaviour is interpreted as circulation, and the resonance is absent. If the libration of the resonant argument is changed by the circulation or *vice versa*, the resonance is defined as unstable (Murray and Dermott, 1999).

To confirm the librating or circulating behaviour of the resonant argument, we can use phase portraits. Visualizing the evolution in the coordinates plane $e\cos\psi$ and $e\sin\psi$, we determine the position of the curve relative to the zero mark. If the curve encompasses the origin of the coordinates, a circulation is observed; another behaviour allows us to speak about the presence of a libration (Murray and Dermott, 1999).

3.4 Algorithm for determining the OMEGNO parameter

To estimate the chaoticity of the asteroid orbit, in addition to the classical MEGNO parameter (Gozdziewski et al., 2001; Cincotta et al., 2003; Valk et al., 2009), the modified OMEGNO (Orthogonal Mean Exponential Growth factor of Nearby Orbit) parameter (Koksin and Shefer, 2014) is used. This parameter has a number of advantages for investigation of the chaoticity of the NEA orbits, because the OMEGNO ($Y_\perp$) parameter not only distinguishes between the chaotic and regular orbits, but also reveals and subdivides the periodic trajectories in the regions of regular motion of continuous dynamic systems.

The MEGNO parameter is based on the vector $\boldsymbol{\delta}$ defining the evolution of initial small deviation $\boldsymbol{\delta}(t_0)$ from the state vector $\mathbf{q} = (\mathbf{x}, \dot{\mathbf{x}})$. The parameter OMEGNO determines an Orthogonal Mean Exponential Growth factor of Nearby Orbits. Its definition is based on the vector $\boldsymbol{\delta}_\perp(t)$ – the component of the vector $\boldsymbol{\delta}(t)$ orthogonal to the phase flow direction at the point $\mathbf{x}(t)$. The algorithm for determining the OMEGNO parameter is described in detail in (Koksin and Shefer, 2014).

Unlike the classical MEGNO parameter, an important role in determining the character of motion using the OMEGNO parameter is played not only by the value $Y_\perp = 2$, but also by $Y_\perp = 0$. For quasiperiodic (regular) orbits, $Y_\perp \to 2$, and it is important to note from what side the parameter approaches 2. If $0 < Y_\perp \leq 2$, the parameter approaches 2 from below, and the trajectory is close to a stable periodic orbit, whereas when the curve approaches 2 from above, the trajectory is close to an unstable periodic orbit. If $Y_\perp > 2$ and grows, on average, linearly, the motion is considered to be chaotic. Finally, $Y_\perp = 0$ for a periodic orbit described by equations of the harmonic oscillator and for any periodic orbit other than that of the harmonic oscillator.

4 Program implementation

The algorithms described in the preceding Section were added to the already available subsystems, and on the basis of some of them, new subsystems were developed.

4.1 Modified Observations subsystem

The *Observations* subsystem has undergone significant changes. The capability to determine the Yarkovsky effect parameters by orbit fitting using the least squares method with allowance for not only positional, but also radar observations of the object was added exactly to this subsystem. In addition, the major planet ephemeris DE438 was added. As an example, Fig. 1 shows the monitor screen of the *Observations* subsystem.

4.2 OMEGNO subsystem

By analogy with the *MEGNO* subsystem, the *OMEGNO* subsystem was developed based on the algorithm for determining the orthogonal chaoticity parameter OMEGNO. For correct program implementation, the input information is required

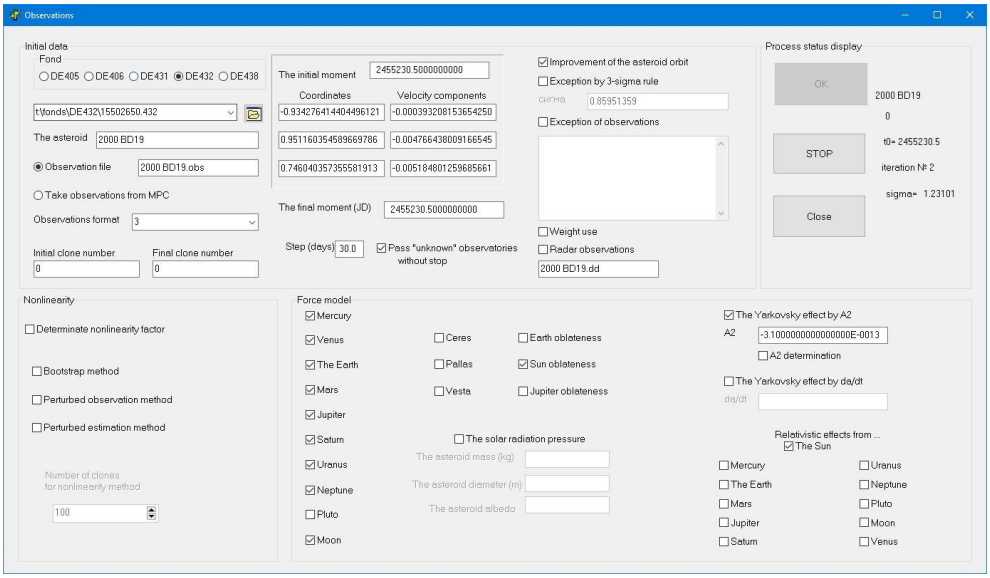


Figure 1 Monitor screen of the *Observations* subsystem.

analogous to that of the *MEGNO* subsystem (Galushina et al., 2019). At the output, the program gives the average OMEGNO parameter and its non-averaged values obtained with a given step. Information on the transition through the critical value 2 is filed separately. The *OMEGNO* subsystem was realized in two variants – for a personal computer and in parallel programming environment.

4.3 Secular resonances subsystem

Based on the algorithm for a search of secular resonances in the asteroid dynamics, the *Secular resonances* subsystem was created in the rapid application development studio (Delphi) to build the evolution of twenty resonant relationships from Table 1 and the resonant arguments corresponding to them during the examined time period. In addition to the main characteristics of the secular resonance, values of the Lidov–Kozai integral $c_1 = (1 - e^2)\cos^2 i$ and the Tisserand relations were calculated in the program for each of the major planets (Bonsor and Wyatt, 2012).

Files with the Keplerian elements or the coordinates and velocity components and the file with values $\dot{\omega}$ and $\dot{\Omega}$ with a given time step were used as input data of the program. These data were provided by the *Evolution* subsystem.

Before the program implementation, it is necessary to assign the following data:

- Ephemeris of the major planets and the path to it;
- System of (equatorial or ecliptic) coordinates in which the input data are given;
- The number of asteroids for which the secular resonances are searched.

At the output, the user receives a number of files containing the following data:

- Resonant relationships (20 variants from Table 1) for interaction with each of the major planets and Pluto;
- Resonant arguments of the resonant relationships from Table 1 for the interaction with each of the major planets and Pluto;
- Values of $e\cos\psi$ and $e\sin\psi$ to visualize the phase portraits of the interaction with each of the major planets and Pluto;
- Values of the Lidov–Kozai integral $c_1 = (1-e^2)\cos^2 i$;
- Values of the Tisserand relation.

Results in the output files are given with the same step as the input data.

The program has passed approbation for objects with various special features of motion. The secular resonances in the asteroid dynamics obtained using the *Secular resonances* subsystem can be found in (Galushina and Sambarov, 2017; Letner and Galushina, 2019; Letner and Galushina, 2020; Galushina and Letner, 2020).

5 Automation of some processes of the orbital evolution of asteroids

When implementing the program complex *IDA*, it is often necessary to repeat some actions several times. These actions are time-consuming, especially if the procedures are executed for large groups of asteroids. In addition, the probability is high that the user, performing constantly repeated operations of the same type, can make this or that error. In this situation, automation of these operations is a good decision. We included the automation of the following processes in the program complex:

- the orbit fitting by the least squares method and generating a clone ensemble (*ida_id*);
- estimation of the influence of the perturbing factors on the asteroid dynamics (*ida_p*);
- adjusting the transverse acceleration component to take into account the Yarkovsky effect (*ida_A2*);
- drawing a large array of graphs.

The programs *ida_id*, *ida_p* and *ida_A2* were written in Delphi. Before implementation of each of them, the required data should be written into the files *input_id.txt*, *input_p.txt* and *input_yar.txt*, respectively. A large array of graphs are drawn using the script developed by the Golden Software Grapher.

Figures 2, 3 and 4 illustrate schematically the stages of program implementation. The stages of implementation of the program *ida_id* are shown in Fig. 2.

As the input data, the data of asteroid observations borrowed from the website of the Minor Planet Center (https://minorplanetcenter.net/) and the Keplerian elements from the E. Bowel catalog were used (Bowell et al., 1994). In the file *input_id.txt*, information on the employed major planet ephemeris, consideration of the perturbing factors, and the list of asteroids were recorded. It is important that the asteroid designations correspond to those in the observation base. After the program launch, the process is automatically repeated for a given number of asteroids. The method of construction of the initial confidence region for an asteroid was described in (Syusina

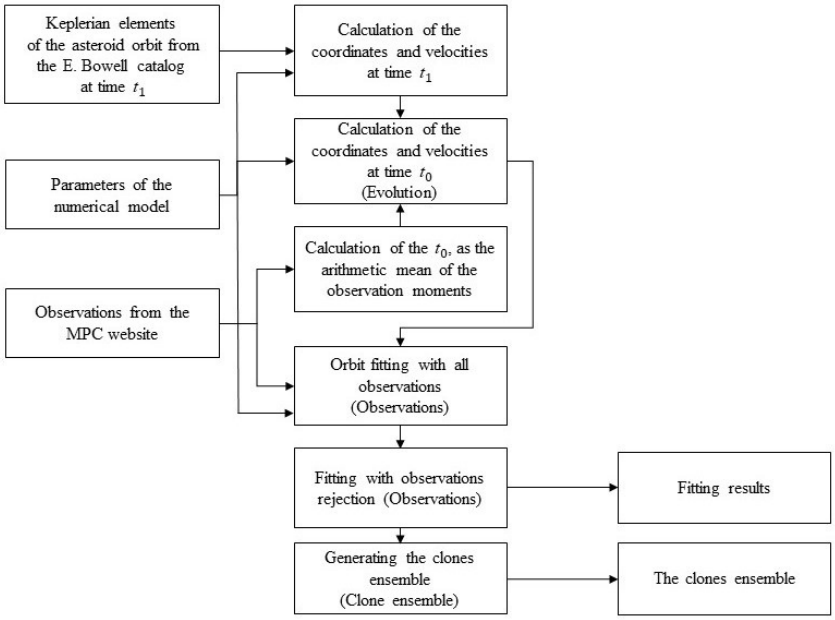


Figure 2 Stages of the process of orbit fitting by the least squares method and generating the clone ensemble.

et al., 2012). In this scheme and in the schemes shown below, the employed subsystem names are written in the parentheses.

Figure 3 shows the stages of the process of estimating the influence of the perturbing factors on the asteroid dynamics in the program *ida_p*. The perturbing factors were estimated using five methods: "Evolution without fitting", "Evolution with fitting", "Acceleration", "Sigma" and "Region". The detailed description of the methods was given in (Galushina et al., 2015; Galushina and Sambarov, 2017).

The procedure of determining A_2 by a search of values from a given interval (see Section 2.1) was implemented in the program *ida_A2*. The problem of adjusting the parameter by minimization of the mean squared error was solved automatically by correcting the parameters of the numerical model and recording the list of asteroids in the file *input_yar.txt* by the scheme shown in Fig. 4.

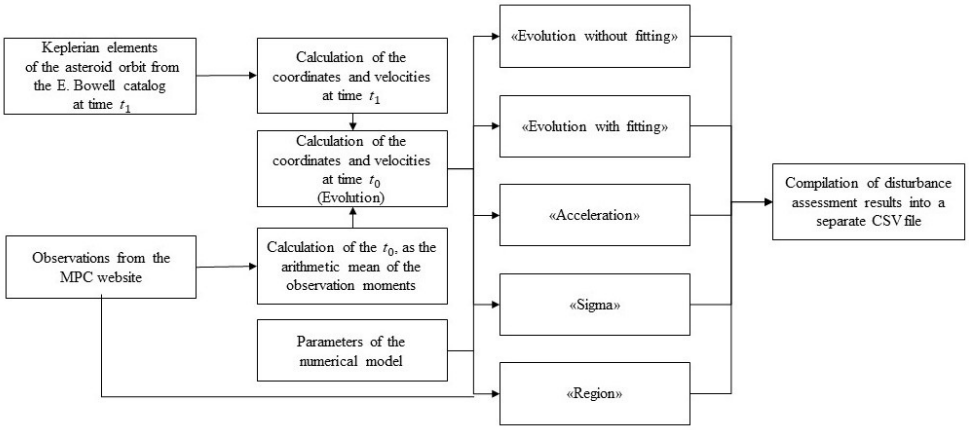


Figure 3 Stages of the process of estimating the influence of the perturbing factors on the asteroid dynamics.

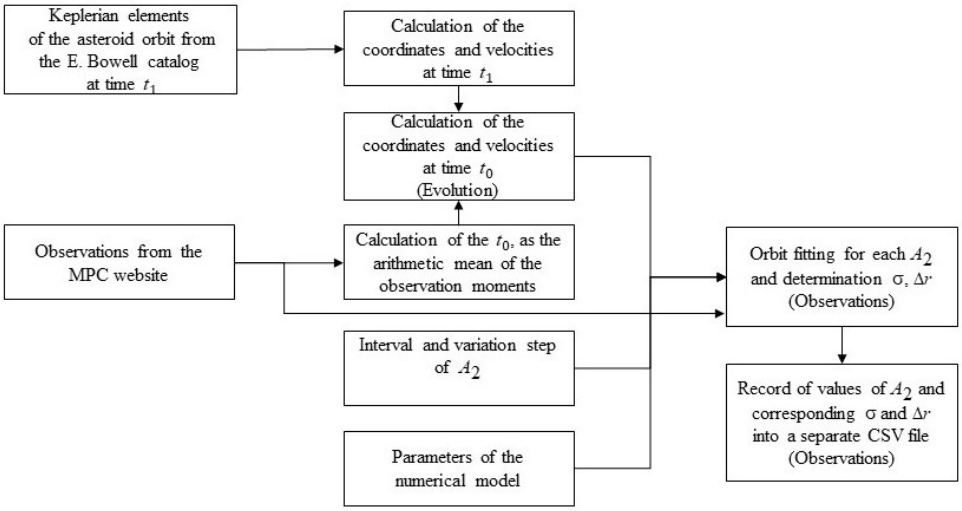


Figure 4 Stages of the process of estimating the influence of the perturbing factors on the asteroid dynamics.

6 Study of the dynamics of asteroid 2007 PR10

The modification of the *IDA* software allowed us to investigate in more detail the dynamics of asteroids with small perihelion distances and to estimate the Yarkovsky effect on their motion. Using the example of asteroid 2007 PR10, this Section presents the results of its orbital evolution obtained using the program complex *IDA*.

The asteroid has a perihelion distance of 0.133 AU and belongs to the class of NEA with the Apollo-type orbit. According to the data of the Minor Planet Center

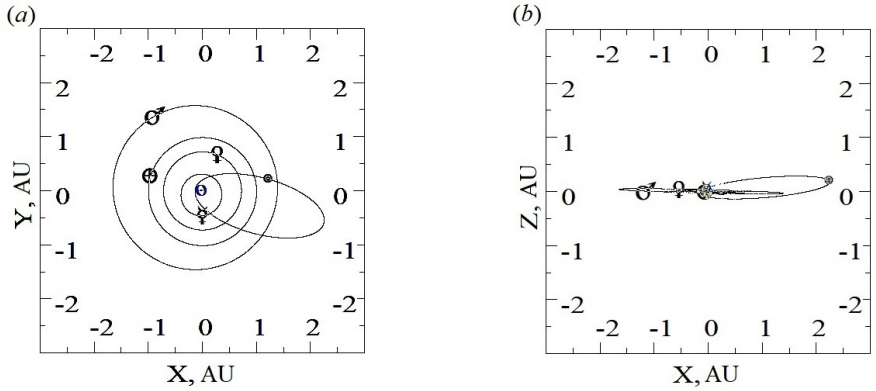


Figure 5 Projection of the orbit of asteroid 2007 PR10 in the heliocentric coordinate system onto the ecliptic plane (a) and onto the plane perpendicular to the ecliptic plane (b).

(https://minorplanetcenter.net/), asteroid 2007 PR10 has 54 observations, which were obtained in two oppositions of the object in 2007 and 2018.

Figure 5 shows two projections of the asteroid orbit in the heliocentric coordinate system: onto the ecliptic plane (a) and onto the plane perpendicular to the ecliptic plane (b). The projections were obtained using the *Assol* subsystem. From graphs (a) and (b) it can be seen that the NEA orbit has an elongated form that can potentially lead to asteroid approaches to the major planets.

To estimate the influence of the Yarkovsky effect on the asteroid dynamics, the results of our studies were compared with the models of forces (including perturbations from the major planets, the Moon, three large Ceres, Pallas and Vesta asteroids, relativistic effects of the Sun and the Sun oblateness) with and without the YE. The forces' model was adjusted by analyzing the results obtained automatically using the program *ida_p* for estimating perturbations. The coefficient A_2 of the Yarkovsky effect was determined by minimization of the mean squared error by including the coefficient A_2 into the list of the estimated parameters when solving the least squares problem.

During the time period of (–6000, 5500) years, the probabilistic orbital evolution of the asteroid was studied with and without the Yarkovsky effect. The study of the probabilistic orbital evolution included two main stages: the construction of the initial confidence region and tracking the evolution of the nominal particle and clones. The initial confidence region of the asteroid was constructed automatically based on the results of analysis of observations using the program *ida_id*. The orbital evolution of the nominal particle and 9984 clones for the chosen forces' model was studied on the TSU supercomputer using the *Evolution* subsystem.

Table 2 presents the fitting results of the asteroid orbit with and without the Yarkovsky effect and the value of the coefficient A_2. In both cases, one observation was excluded from consideration. From Table 2 it follows that the Yarkovsky effect reduced the mean squared error σ and the mean squared error of the LSM (least squares method) estimate $\sigma(x_0)$ of the asteroid position vector.

Table 2 Data of observations, fitting results of the asteroid orbit and value of the employed coefficient A_2 with and without the Yarkovsky effect.

	N	Δt, days	A_2, AU/day^2	$\sigma,''$	$\sigma(\mathbf{x}_0)$, AU
Without YE	53	4020	0	0.388	$7.554 \cdot 10^{-6}$
With YE	53	4020	$-3.866 \cdot 10^{-13}$	0.374	$7.280 \cdot 10^{-6}$

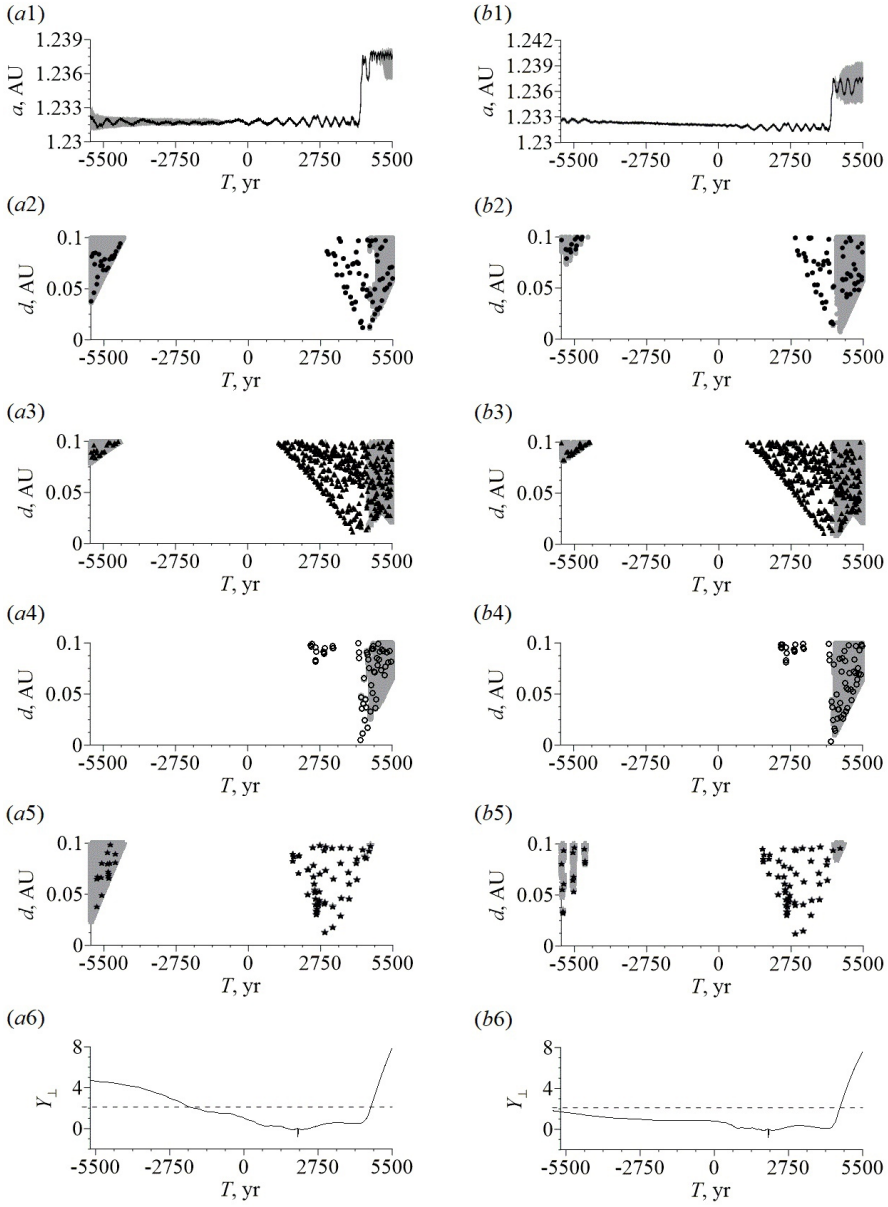


Figure 6 Orbital evolution of asteroid 2007 PR10 without (a) and with (b) the Yarkovsky effect.

The approaches of the asteroid to all inner planets (Mercury, Venus, the Earth and Mars) were detected, and the orbit chaoticity was estimated using the OMEGNO parameter (the *OMEGNO* subsystem). Figure 6 illustrates the evolution of some orbital parameters without (a) and with (b) the Yarkovsky effect. Here graphs $a1$ and $b1$ show the evolution of the semimajor axis a, graphs $a2$ and $b2$ show the approaches to the Earth (•), graphs $a3$ and $b3$ show the approaches to Mercury (Δ), graphs $a4$ and $b4$ show the approaches to Venus ($\circ$), graphs $a5$ and $b5$ show the approaches to Mars (*), and graphs $a6$ and $b6$ show the evolution of the OMEGNO parameter.

Our study showed that the evolution of the Keplerian elements of the 2007 PR10 orbit differed insignificantly for two models of forces, except for the semimajor axis a. As can be seen from graphs $a1$ and $b1$ (Fig. 6), the Yarkovsky effect changed noticeably the semimajor axis and thereby influenced the number of approaches and the distance to the planets. During integration into the future for the nominal particle with the Yarkovsky effect the precision is significantly lower, and the confidence region started to increase earlier than without the Yarkovsky effect. From graph $b4$ in Fig. 6 it can be seen that the asteroid approached closer to Venus, and then the confidence region started to grow. The opposite pattern is observed for integration into the past. Without the Yarkovsky effect, the confidence region started to grow earlier.

The evolution of the parameter OMEGNO (graphs $a6$ and $b6$) for two forces' models is similar for integration into the future and differs considerably for integration into the past. In future, the asteroid will approach repeatedly and more closely to Mercury, Venus, the Earth and Mars. After a group of the closest approaches to the planets, the parameter OMEGNO started to grow, on average, linearly, that is, the asteroid orbit showed signs of chaoticity.

Integration into the past without the Yarkovsky effect results in a greater number of asteroid approaches to the Earth and Mars and more close approaches to the Earth. Before 1960, the asteroid orbit showed signs of chaoticity. With the Yarkovsky effect, the asteroid motion in the past remained regular. It should be noted that the start of growth of the confidence region correlated with the increase of the parameter OMEGNO, that is, with signs of chaoticity in the asteroid motion.

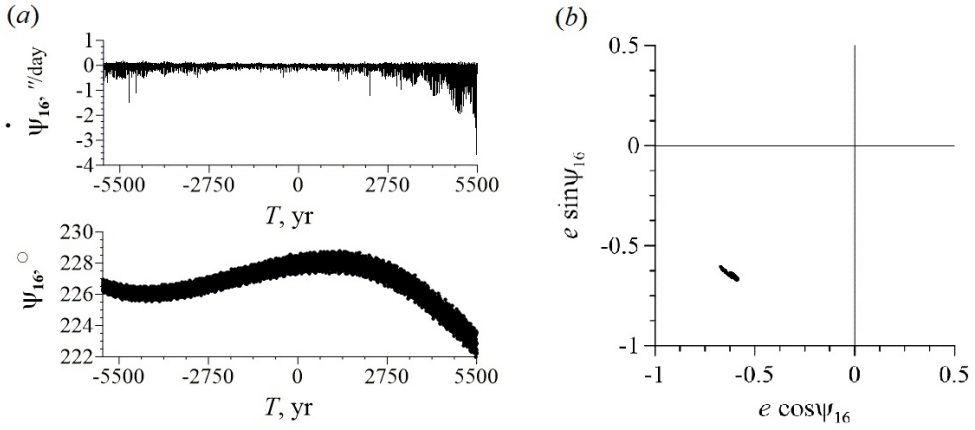


Figure 7 Behaviour of the resonant characteristics of secular resonance No. 16 of asteroid 2007 PR10 with Venus: the evolutions of the resonant relationship $\dot{\psi}$ and the corresponding resonant argument ψ (a) and the phase portrait of the resonant argument (b).

The search for the secular resonances in the dynamics of asteroid 2007 PR10 during the time period of (–6000, 5500) years was carried out using the *Secular resonances* subsystem and the results of investigation of the orbital evolution (the *Evolution* subsystem). The results of our study demonstrated that during this time period, the arguments of all 20 relationships from Table 1 changed within 360°, and the relationships oscillated around the zero value. In spite of the fact that the integration period appeared insufficient to identify the period and the amplitude of oscillations of the resonant argument, the presence and stability of resonances during the examined time period can be judged from the behaviour of the resonant characteristics. It is important to note that the Yarkovsky effect did not influence the character of the behaviour of the resonant characteristics.

As an example, Fig. 7 shows the graphs illustrating the behaviour of the resonant characteristics and the phase portrait for the resonance $\dot{\psi}_{16}$ with Venus.

7 Conclusions

Thus, the *IDA* software has been modified, which allowed the asteroid motion to be more accurately predicted. The algorithms for determining the Yarkovsky effect parameter and its consideration in the study of the orbital evolution of asteroids were added to the program complex together with the capability of processing radar observations. In addition to the added algorithms, new subsystems *OMEGNO* and *Secular resonances* were developed to deepen our understanding and to reveal new peculiarities of asteroid motion.

To decrease the computational time for solving problems of the same type and to avoid errors connected with the human factor, the processes of orbit fitting and initial-confidence regions' constructing have been automated together with estimations of the influence of the perturbing factors on the asteroid dynamics and adjustment of the transverse acceleration component of the Yarkovsky effect. To draw large arrays of graphs, a script developed by the Golden Software Grapher was used.

The orbital evolution of asteroid 2007 PR10 with small perihelion distance has been studied using the modified software with and without the Yarkovsky effect. It was shown that the effect influences the evolution of the semimajor axis of the asteroid, thereby leading to changes in the number of approaches and the distances to the planets. As a consequence of such changes in the orbital evolution, the confidence region of 2007 PR10 behaved differently. The signs of chaoticity in asteroid motion were studied using the parameter OMEGNO, and all apsidal-nodal resonances to the 6th order inclusive were revealed.

Acknowledgemengts

This work was supported by the Russian Science Foundation (Project No. 19-72-10022). The research made use of NASA's Astrophysics Data System, Scopus (Elsevier), and the Minor Planet Center.

References

Aleksandrova A.G., Bordovitsyna T.V., Popandopulo N.A., Tomilova I.V. (2020) Russian Physics Journal 63(1), 64
Bonsor A., Wyatt M.C. (2012) MNRAS 420(4), 2990
Bordovitsyna T.V., Tomilova I.V., Chuvashov I.N. (2012) Sol. Syst. Res. 46 (5), 329
Bordovitsyna T.V., Tomilova I.V., Chuvashov I.N. (2014) Sol. Syst. Res. 48 (4), 259
Bowell E., Muinonen K., Wasserman L.H. (1994) In Asteroids, Comets, Meteors, Kluwer, Dordrecht, Netherlands, 477
Chirikov B.V. (1979) Phys. Rep. (Rev. Sect. Phys. Lett.) 52 (5), 263
Cincotta P.M. et al. (2003) Physica D 182, 151
Farnocchia D., Chesley S.R., Vokrouhlicky D., et al. (2013) Icarus 224, 1
Galushina T.Yu., Syusina O.M. (2020) Russian Physics Journal 63(3), 420
Galushina T., Bykova L., Letner O., Baturin A. (2019) Astronomy and Computing 29, id. 100301
Galushina T.Yu., Letner O.N. (2020) Russian Physics Journal 63(1), 71
Galushina T.Yu., Ryabova G.O., Skripnichenko P.V. (2015) Planetary and Space Science 118, 296
Galushina T.Yu., Sambarov G.E. (2017) Planetary and Space Science 142, 38
Gozdziewski K., Bois E., Maciejewski A.J., et al. (2001) Astron. Astrophys 378, 569
Koksin A.M., Shefer V.A. (2014) Proc. IAU Symp. No. 310 (Complex Planetary Systems) 9, 35
Letner O. N., Galushina T. Yu. (2019) Solar System Research 53(1), 20
Letner O. N., Galushina T. Yu. (2020) Planetary and Space Science 181, id. 104818
L'vov V. N., Tsekmeister S. D. (2012) Solar System Research 46(2), 177
Murray C.D., Dermott S.F. (1999) Solar system dynamics. Cambridge: Cambridge University Press, 592
Novikov F. A., Shor V. A., Vega T. G. , et al. (2009) Protecting the Earth against Collisions with Asteroids and Comet Nuclei, Proceedings of the International Conference "Asteroid-Comet Hazard 2009", ed. A.M. Finkelstein, W.F. Huebner, V.A. Shor (St. Petersburg: Nauka), 32
Syusina O.M., Chernitsov A.M., Tamarov V.A. (2012) Solar System Research 46(3), 195
Valk S. et al. (2009) Adv. Space Res. 43, 1509
Yeomans D.K. et al. (1992) The Astronomical Journal 103(1), 303